



Rare earth complexes chemiluminescence catalyzed by gold nanoparticles for fast sensing of Tb³⁺ and Eu³⁺

Jiajia Yuan, Xiaoya Fan, Jiacheng Yang, Xinfeng Zhang*

State Key Lab of Geohazard Prevention & Geoenvironment Protection, College of Materials and Chemistry & Chemical Engineering, Chengdu University of Technology, Chengdu 610059, China

ARTICLE INFO

Article history:

Received 23 August 2022
Revised 7 January 2023
Accepted 18 January 2023
Available online 26 January 2023

Keywords:

Gold nanoparticles
Rare earth ions
Chemiluminescence
Multiplex analysis
Fast sensing

ABSTRACT

Developing multiplex sensing technique is of great significance for fast sample analysis. However, the broad emissions of most chemiluminescence (CL) luminophores make the multiplex CL analysis be difficult. In this work, a simple and sensitive CL analytical method has been developed for the simultaneous determination of Tb³⁺ and Eu³⁺ thanks to their narrow band emission. The technique was based on a mixed CL system of periodate (IO₄⁻)-hydrogen peroxide (H₂O₂)-rare earth complexes, in which the reactive oxygen species (ROSs) especially singlet oxygen (¹O₂) can transfer its energy to the complex of Tb³⁺/Eu³⁺-ethylenediaminetetraacetic acid disodium salt (EDTA) and then produce the characteristic emissions of Tb³⁺ and Eu³⁺ without cross-interference. The further experiment found that the CL emissions of Tb³⁺ and Eu³⁺ could be catalyzed by the gold nanoparticles (AuNPs) via enhancing the yield of ¹O₂. The CL intensities of Tb³⁺ (at 490 nm) and Eu³⁺ (at 620 nm) increased linearly with concentration of Tb³⁺ and Eu³⁺. After the optimization of the CL sensing conditions, the limits of detection (LOD) were 5.0 × 10⁻⁹ mol/L and 8.0 × 10⁻⁷ mol/L for Tb³⁺ and Eu³⁺, respectively. Finally, the method has been applied for measuring the contents of Tb³⁺ and Eu³⁺ in leaching solution of mine sample and Tb³⁺/Eu³⁺-containing nanomaterials with satisfactory results. The present system provides a new CL technique for multiplex sensing with simplicity and high sensitivity.

© 2023 Published by Elsevier B.V. on behalf of Chinese Chemical Society and Institute of Materia Medica, Chinese Academy of Medical Sciences.

Chemiluminescence (CL) accompanying with light emission by the chemical reaction, displays the merits of high sensitivity, wide linear range and low background signal. It has been widely used in food analysis [1,2], environmental monitoring [3,4] and chem-/biosensing [5], *etc.* The common CL systems include luminol [6,7], peroxyoxalate [8–10], potassium permanganate [11,12], cerium [13,14], periodate [15,16], *etc.* However, most of these CL systems are based on the emission of molecular luminophore. The broad emission band of molecular luminophore makes multi-component analysis be difficult. Hence, developing a new CL system that can achieve multiple components is still highly desired.

In recent years, rare earth elements (REEs) have attracted widespread interest owing to their unique properties. The photoluminescence properties of lanthanide ions (Ln³⁺) mostly come from the f→f transitions of its 4f orbitals, which are well shielded from the environment by the outer 5s² and 5p⁶ shells. Importantly, the Ln³⁺ ions are usually characterized by narrow band emission, large Stokes shifts and long luminescence lifetime [17–

19]. Thus, the narrow band emission of Ln³⁺ ions makes it promising for multi-component analysis. In most cases, the Ln³⁺ excitation was achieved by light source [20–22]. The background of the light sources can usually deteriorate the sensing sensitivity.

Recently, chemoexcitation has demonstrated to be promising for the excitation of fluorophore [23,24], quantum dots [25], *etc.*, since CL excitation can avoid light background and improve the signal-to-noise ratio during detection [2]. In recent years, REE ions especially Tb³⁺ and Eu³⁺ were also successfully chemoexcited by reaction system such as oxalate-hydrogen peroxide (H₂O₂), SO₃²⁻-Eu/CeO₂, periodate (IO₄⁻)-H₂O₂ [26–29]. Among them, IO₄⁻ was the mostly used as the oxidant since it is water-soluble and colourless which evades the emission absorption problems [30,31]. Nevertheless, the simultaneous excitation of Tb³⁺ and Eu³⁺ by the CL reaction system has not been studied. Additionally, the relatively weak CL emission from Tb³⁺/Eu³⁺-based CL systems limits their applications in chemo/bio-sensing.

Hence, in this work, we demonstrate the simultaneous excitation of Tb³⁺ and Eu³⁺ by IO₄⁻-H₂O₂ CL reaction, and the analytical procedure is shown in Fig. S1 (Supporting information). The reactive oxygen species (ROSs) especially singlet oxygen (¹O₂) that generated by IO₄⁻-H₂O₂ system can transfer its energy to the com-

* Corresponding author.

E-mail address: zhangxinfeng09@cdut.cn (X. Zhang).

plex of $\text{Tb}^{3+}/\text{Eu}^{3+}$ -ethylenediaminetetraacetic acid disodium salt (EDTA), then producing the CL emissions of Tb^{3+} and Eu^{3+} . More importantly, the emissions can be further enhanced by the catalysis of gold nanoparticles (AuNPs). The resulted strong characteristic CL emissions of Tb^{3+} at 490 nm and Eu^{3+} at 620 nm allow sensitive and simultaneous detection of Tb^{3+} and Eu^{3+} . This AuNPs-catalyzed rare earth complexes CL system provides a new CL technique for multiplex sensing with simplicity and high sensitivity.

As shown in Fig. 1A, Tb^{3+} cannot yield CL emission in the presence of NaIO_4 , H_2O_2 or EDTA alone, and even in the CL reaction between NaIO_4 and H_2O_2 ; the characteristic CL emissions of Tb^{3+} appear only in the presence of NaIO_4 , H_2O_2 and EDTA. It indicates that EDTA plays an important role in the luminescence of Tb^{3+} , which can be attributed to the antenna effect of ligands [32,33].

Luminescence is an important property of rare earth ions, so we further verify whether other rare earth ions could also produce CL in this investigated system. The investigated ions include La^{3+} , Ce^{3+} , Pr^{3+} , Nd^{3+} , Sm^{3+} , Dy^{3+} , Er^{3+} , Eu^{3+} and Gd^{3+} . It can be seen in Fig. 1B, only Tb^{3+} , Eu^{3+} and Dy^{3+} produce obvious CL emissions with Tb^{3+} being the strongest, Eu^{3+} the second strongest and Dy^{3+} the smallest. This may be attributed to the difference in energy transfer efficiency between EDTA and these investigated ions, because only Tb^{3+} , Eu^{3+} and Dy^{3+} also produce characteristic emissions in the fluorescence experiments (Fig. S2 in Supporting information). Although the emission peaks of Tb^{3+} and Dy^{3+} overlap at 490 nm, the intensity of 1 mmol/L Tb^{3+} is much higher than that of 5 mmol/L Dy^{3+} . Since the high CL emissions of Tb^{3+} and Eu^{3+} -EDTA complexes, so we use the CL system for multiplex detection of Tb^{3+} and Eu^{3+} .

The results in Fig. 1A show that ligand is critically important for the CL process of Tb^{3+} . Therefore, we studied the sensitization role of a variety of ligands in Tb^{3+} and Eu^{3+} CL emissions, including EDTA, 2'-deoxyadenosine 5'-triphosphate trisodium salt (ATP), diethylenetriamine-pentaacetic acid (DTPA), sulfosalicylic acid dehydrate (SAD), L-cysteine hydrochloride monohydrate (Cys), 2,6-pyridinedicarboxylic acid (DPA) and enrofloxacin (ENX). As depicted in Fig. 1C, the three ligands (EDTA, ATP and DTPA) can produce strong CL emissions from the NaIO_4 - H_2O_2 - $\text{Tb}^{3+}/\text{Eu}^{3+}$ systems under their optimal conditions, the CL curves of Tb^{3+} and Eu^{3+} with a variety of ligands were shown in Fig. S3 (Supporting information). And EDTA was selected for subsequent experiments by considering the stability of the complexes as well as the cost effectiveness.

In recent years, the enhancement of CL by the catalysis of Au NPs has been studied [34–36], hence we also intend to explore whether AuNPs can contribute to the CL emissions of Tb^{3+}

and Eu^{3+} . The synthetic AuNPs were characterized by transmission electron microscopy (TEM), ultraviolet-visible (UV-vis) spectrophotometer and X-ray Photoelectron Spectroscopy (XPS). The data in Fig. 2A revealed that they are spherical particles with an average diameter of about 13 nm and the UV absorption peak at 520 nm was illustrated in Fig. S4 (Supporting information). The overall XPS survey shows the presence of strong C 1s, O 1s and Au 4f core levels of citrate capped AuNPs (Fig. S5 in Supporting information). In Fig. 2B, we found that the presence of AuNPs in the NaIO_4 - H_2O_2 -EDTA- Tb^{3+} solution caused an obvious enhancement in the CL emission. And AuNPs also has a catalysis effect on Eu^{3+} CL emission (Fig. S6 in Supporting information).

The reaction of IO_4^- with H_2O_2 may involve the generation of ROSs, such as hydroxyl radicals ($\cdot\text{OH}$) and superoxide anion ($\cdot\text{O}_2^-$) [31,37,38] which are important for the CL. This was confirmed by free radical scavenging experiments (Fig. S7 in Supporting information) and room temperature electron paramagnetic resonance (EPR) analysis (Figs. 2C-E), which indicated that three free radicals ($\cdot\text{OH}$, $\cdot\text{O}_2^-$ and $^1\text{O}_2$) are indeed generated in the NaIO_4 - H_2O_2 system. Furthermore, it found that the addition of AuNPs to the NaIO_4 - H_2O_2 system resulted in significantly increasing signals for 2,2,6,6-tetramethylpiperidinoxy (TEMPO) adduct (Fig. 2E), suggesting that AuNPs could promote the production of $^1\text{O}_2$. It is generally believed that oxidation of H_2O_2 by IO_4^- generates excited singlet oxygen molecular pair [$(^1\text{O}_2)_2^*$], which then produces a CL emission [31,39]. So we have further explored the effect of AuNPs on the production of $^1\text{O}_2$ using 1,3-diphenylisobenzofuran (DPBF) as an indicator. From Fig. 2F, it can be concluded that AuNPs indeed contribute to the production of $^1\text{O}_2$ because UV absorption of DPBF is reduced more seriously in the presence of AuNPs. These results indicated the good catalytic activity of AuNPs for enhanced generation of $^1\text{O}_2$ in the investigated CL system.

For the catalytic effect of AuNPs, it is generally believed that the O–O bond of H_2O_2 might be broken up into double $\cdot\text{OH}$ radicals and these radicals were further stabilized by AuNPs *via* partial electron exchange interactions [40]. And the generated $\cdot\text{OH}$ reacted with H_2O_2 to facilitate the formation of HO_2^{\cdot} , which immediately dissociated into $\cdot\text{O}_2^-$ at high pH values [41]. Additionally, $\cdot\text{OH}$ and $\cdot\text{O}_2^-$ radicals could also be generated from the reaction of IO_4^- with dissolved O_2 . $^1\text{O}_2$ could be produced from the reaction of H_2O_2 or ROSs (e.g. $\cdot\text{O}_2^-$ or $\cdot\text{OH}$) with IO_4^- [42].

It has been reported that $^1\text{O}_2$ can transfer its energy to fluorescent substances by the intermolecular energy transfer process [43,44]. However, lanthanide $4f^N-4f^N$ transitions are Laporte forbidden, and the direct excitation of electrons in tripositive lanthanide ions is inefficient. Hence, a sensitizing chromophore is

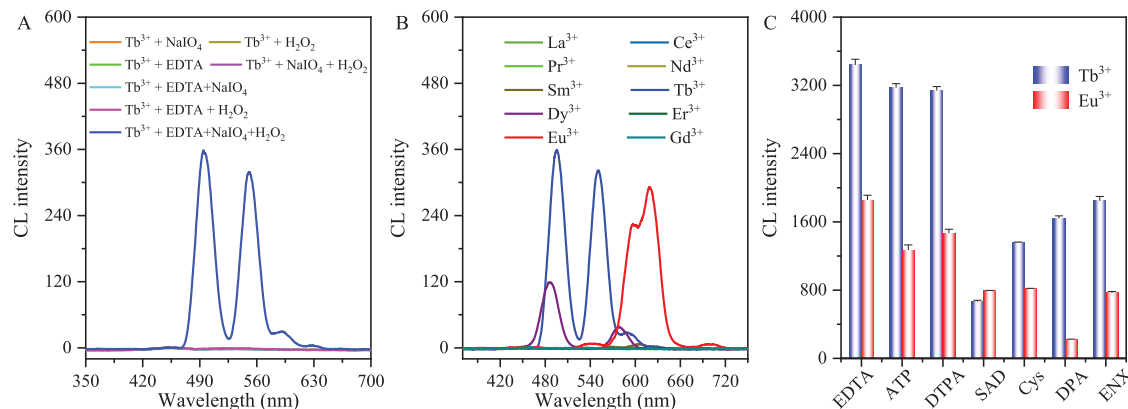


Fig. 1. (A) Sensitization CL of Tb^{3+} . (B) CL of various rare earth ions. (C) CL of different ligands in Tb^{3+} and Eu^{3+} system. Experimental conditions: NaIO_4 , 24 mmol/L; H_2O_2 , 18 mmol/L; EDTA, 35 mmol/L; all the ion are 5 mmol/L in (A and B), except for Tb^{3+} , 1 mmol/L. In (C), NaIO_4 , 8–18 mmol/L; H_2O_2 , 10.67–48 mmol/L; Tb^{3+} , 1 $\mu\text{mol/L}$; ligands, 0.2–13 mmol/L in Tb^{3+} ; NaIO_4 , 10–16 mmol/L; H_2O_2 , 8–30 mmol/L; Eu^{3+} , 20 $\mu\text{mol/L}$; ligands, 0.2–6.67 mmol/L in Eu^{3+} .

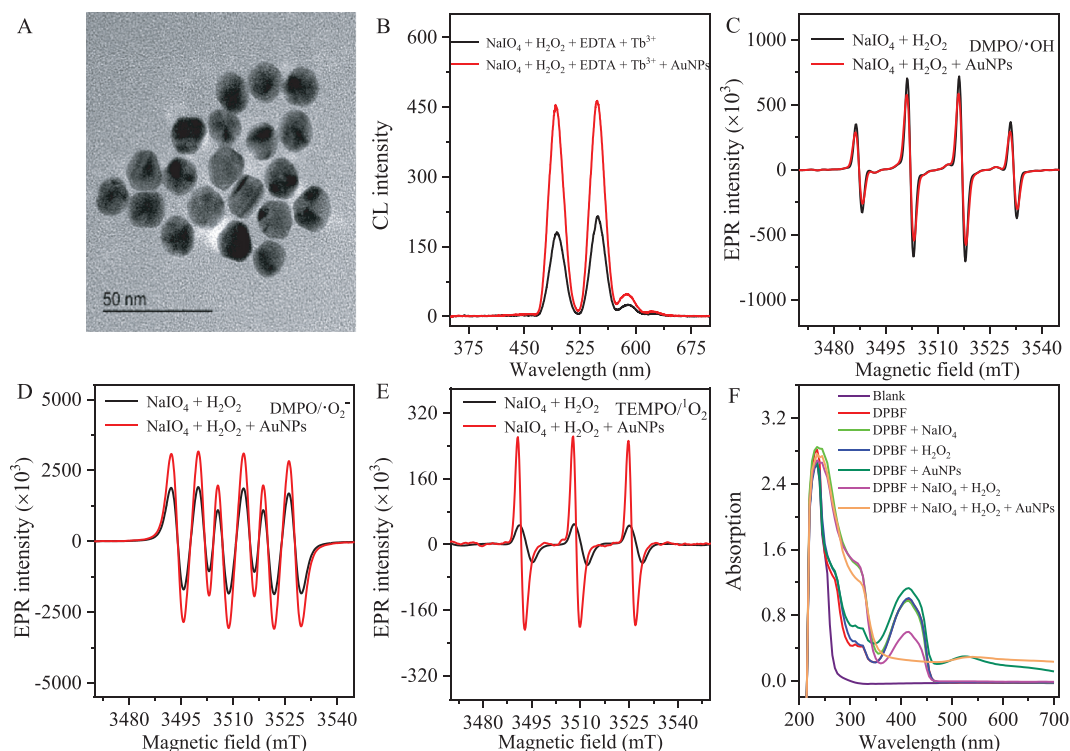


Fig. 2. (A) TEM of synthetic AuNPs. (B) The effect of AuNPs on the reaction of $\text{NaIO}_4\text{-H}_2\text{O}_2\text{-EDTA-Tb}^{3+}$. (C) $\text{DMPO}/\cdot\text{OH}$ adduct in $\text{NaIO}_4\text{-H}_2\text{O}_2$ system in the absence or presence of AuNPs. (D) $\text{DMPO}/\cdot\text{O}_2^-$ adduct in $\text{NaIO}_4\text{-H}_2\text{O}_2$ system in the absence or presence of AuNPs. (E) $\text{DMPO}/^1\text{O}_2$ adduct in $\text{NaIO}_4\text{-H}_2\text{O}_2$ system in the absence or presence of AuNPs. (F) DPBF detection of $^1\text{O}_2$ in presence of AuNPs. Experimental conditions: TbCl_3 , 1 mmol/L; EDTA, 35 mmol/L; H_2O_2 , 18 mmol/L; NaIO_4 , 24 mmol/L; AuNPs, 2 nmol/L and DPBF, 200 $\mu\text{mol/L}$.

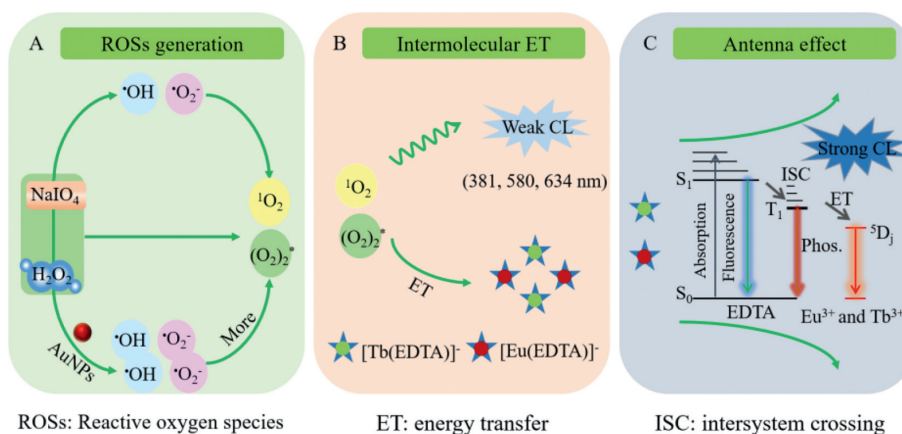


Fig. 3. Possible chemiluminescence reaction mechanism. (A) Reaction between NaIO_4 and H_2O_2 to produce ROSs, (B) intermolecular energy transfer processes between $^1\text{O}_2$ and rare earth complexes, and (C) Antenna effect between ligands and rare earth ions.

usually used as a ligand to chelate to the emissive lanthanide center [18,19]. In such case, the rare earth ion can be excited by the antenna effect. So in this work, the fluorescence quantum yield of Tb^{3+} is greatly enhanced through an intramolecular energy transfer when it forms complexes with EDTA (Fig. 1A).

Hence, the AuNPs-catalyzed CL mechanism of the rare earth complex can be concluded as in Fig. 3: (i) AuNPs catalyzed the production of $^1\text{O}_2$ from $\text{NaIO}_4\text{-H}_2\text{O}_2$ system; (ii) the generated $^1\text{O}_2$ transferred its energy to the ligand (i.e., EDTA) to reach the excited state via intermolecular energy transfer effect and (iii) the rare earth ion was excited via the antenna effect from ligand, being followed by $^5\text{D}_4$ emission of Tb^{3+} in the $[\text{Tb}(\text{EDTA})]^-$ complex (Fig. 1C). The catalytic activity of AuNPs was quite stable with a decline about 5.3% in a week.

We verified the feasibility of simultaneous detection of Tb^{3+} and Eu^{3+} by the constructed CL systems. The characteristic peaks of Tb^{3+} and Eu^{3+} are mainly at 490 nm and 540 nm, 595 nm and 610 nm (Fig. 4A), respectively. And Dy^{3+} in concentrations equal to Tb^{3+} (0.5 mmol/L) produces nearly no luminescence. More importantly, these characteristic peaks (490 nm for Tb^{3+} and 610 nm for Eu^{3+}) do not mutually interfere in the mixed CL system of $\text{NaIO}_4\text{-H}_2\text{O}_2\text{-Tb}^{3+}\text{-Eu}^{3+}\text{-EDTA}$. Hence, the CL system enables multiplex detection of Tb^{3+} and Eu^{3+} .

Some parameters that affect the CL emission were examined, including the concentrations of CL reagents and the pH of solutions (Figs. S8–S12 in Supporting information). Under optimal conditions, the linear response range of $\text{NaIO}_4\text{-H}_2\text{O}_2\text{-EDTA-AuNPs}$ for Tb^{3+} and Eu^{3+} were depicted in Figs. 4B and C. It revealed that the CL intensity of $\text{NaIO}_4\text{-H}_2\text{O}_2\text{-EDTA-AuNPs}$ was gradually en-

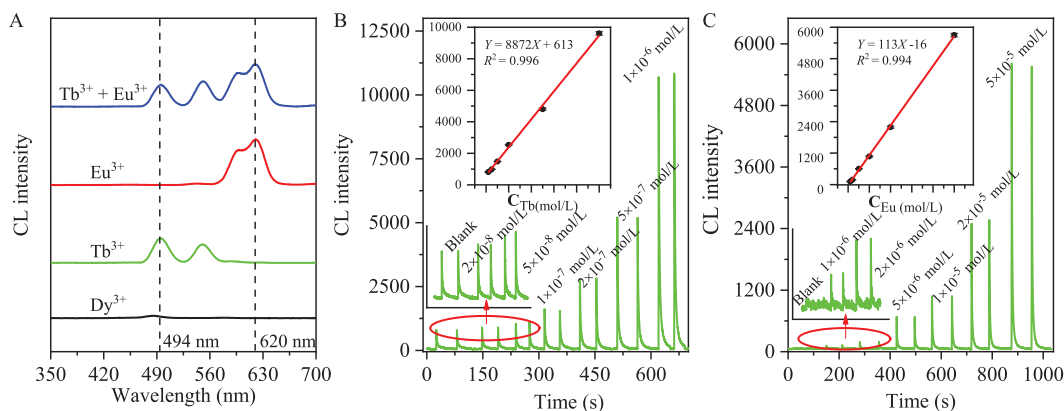


Fig. 4. (A) Construction of a multi-component luminescent system. (B) The standard curves and detection limits of Tb^{3+} . (C) The standard curves and detection limits of Eu^{3+} . Experimental conditions: (A) Tb^{3+} , 0.5 mmol/L; Dy^{3+} , 0.5 mmol/L; Eu^{3+} , 4 mmol/L; EDTA, 35 mmol/L; H_2O_2 , 18 mmol/L and NaIO_4 , 4 mmol/L. (B) EDTA, 13 mmol/L; H_2O_2 , 10.67 mmol/L; NaIO_4 , 13 mmol/L; AuNPs, 2 nmol/L and 480 nm filter. (C) EDTA, 13 mmol/L; H_2O_2 , 10.67 mmol/L; NaIO_4 , 13 mmol/L; AuNPs, 2 nmol/L and 620 nm filter.

hanced with the increase of the Tb^{3+} concentration, and the linear response is ranging from 2.0×10^{-8} mol/L to 1.0×10^{-6} mol/L ($R^2 = 0.9941$). And the CL intensity is also enhanced linearly with increasing Eu^{3+} concentration in the range of 1.0×10^{-6} mol/L to 5.0×10^{-5} mol/L ($R^2 = 0.9967$). The limits of detection (LOD) were calculated to be 5.0×10^{-9} mol/L and 8.0×10^{-7} mol/L for Tb^{3+} and Eu^{3+} respectively (3σ). Notably, the $\text{NaIO}_4\text{-H}_2\text{O}_2\text{-EDTA-AuNPs}$ CL system is much more sensitive than the corresponding fluorescence detection shown in Fig. S13 (Supporting information), in which the LODs for Tb^{3+} and Eu^{3+} were 6.7×10^{-6} mol/L and 2.1×10^{-5} mol/L, respectively. The results of comparing with other methods for the detection of Tb^{3+} and Eu^{3+} are summarized in Table S1 (Supporting information). These results showed that the $\text{NaIO}_4\text{-H}_2\text{O}_2\text{-EDTA-AuNPs}$ system had good linearity, high sensitivity and reproducibility.

To estimate the selectivity of the sensing system, we measured a variety of potentially interfering metal ions on the effect of the system, including Sm^{3+} , Dy^{3+} , Gd^{3+} , Ce^{3+} , Nd^{3+} , La^{3+} , Fe^{3+} , Al^{3+} , Zn^{2+} , Ni^{2+} , Co^{2+} , Mg^{2+} and Cu^{2+} . Fig. S14 (Supporting information) demonstrated that only Tb^{3+} and Eu^{3+} can produce strong CL emission, negligible CL intensities were observed for other metal ions at the same concentrations. And the typical metal ions were further used to investigate the anti-interference ability of the system. As shown in Figs. 5A and B, the CL signals for 0.5 $\mu\text{mol/L}$ Tb^{3+} and 20 $\mu\text{mol/L}$ Eu^{3+} were affected weakly by the examined ions. And for the determination of Tb^{3+} , the tolerable concentration ratios for interference at the 10% level were over 1000 for K^+ , Na^+ and NH_4^+ ; 200 for La^{3+} , 100 for Al^{3+} and Gd^{3+} , 50 for Ce^{3+} and Eu^{3+} , 10 for Mg^{2+} , Fe^{3+} , Ni^{2+} , Cu^{2+} and Sm^{3+} , 5 for Co^{2+} and Dy^{3+} . With respect to Eu^{3+} , the tolerable limit could reach more than 330 times for K^+ , Na^+ and NH_4^+ , 20 for Mg^{2+} , La^{3+} , 13 for Al^{3+} , 6 for Ni^{2+} , Fe^{3+} , Ce^{3+} and Gd^{3+} , 3 for Co^{2+} , Cu^{2+} and Dy^{3+} . And the same concentration of Sm^{3+} and Tb^{3+} has no effect on CL of Eu^{3+} . Hence, the CL system has good selectivity and anti-interference ability.

The applicability for real sample analysis was verified by determination of Tb^{3+} and Eu^{3+} in leaching solution of mine sample. Also, the Tb^{3+} and Eu^{3+} contents in Metal-organic frameworks (MOFs) materials were assessed by this sensing system. In Table 1, the measured values of Tb^{3+} and Eu^{3+} in the samples were in good agreement with those obtained by inductively coupled plasma mass spectrometry (ICP-MS). Hence, the system was practical for real sample analysis.

In summary, rare earth complexes CL system that can catalyzed by AuNPs was developed for fast sensing of Tb^{3+} and Eu^{3+} . The $^1\text{O}_2$ generated from $\text{NaIO}_4\text{-H}_2\text{O}_2$ system can transfer its energy to

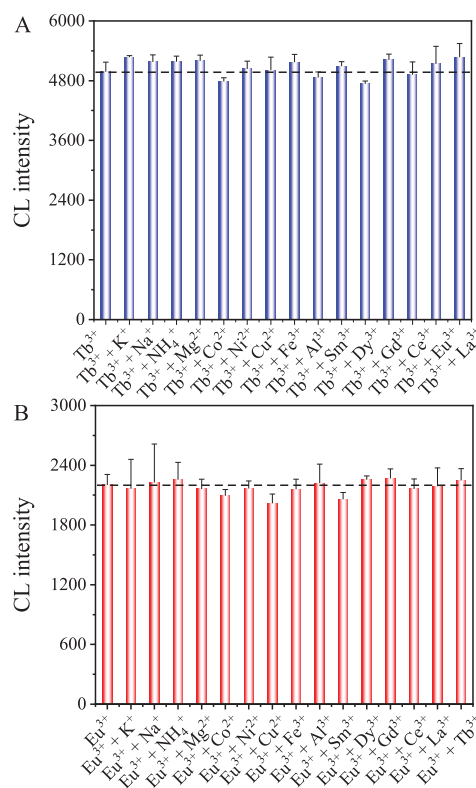


Fig. 5. Anti interference experiment. (A) $\text{NaIO}_4\text{-H}_2\text{O}_2\text{-EDTA-Tb}^{3+}$. (B) $\text{NaIO}_4\text{-H}_2\text{O}_2\text{-EDTA-Eu}^{3+}$. Experimental conditions: EDTA, 13 mmol/L; H_2O_2 , 10.67 mmol/L; NaIO_4 , 13 mmol/L; AuNPs, 2 nmol/L; Tb^{3+} , 0.5 $\mu\text{mol/L}$, interference ions, 0.5–33 $\mu\text{mol/L}$ and 480 nm filter in (A). EDTA, 13 mmol/L; H_2O_2 , 10.67 mmol/L; NaIO_4 , 13 mmol/L; AuNPs, 2 nmol/L; Eu^{3+} , 20 $\mu\text{mol/L}$, interference ions, 20–3000 $\mu\text{mol/L}$, 620 nm filter in (B).

Table 1
Determination of Tb^{3+} and Eu^{3+} in samples.

Samples	Tb (mg/g)		Eu (mg/g)	
	ICP-MS	This method	ICP-MS	This method
Leaching solution of mine sample	0.0016	0.0015 ± 0.0001	0.0036	N.D.
Tb-BTC MOF	10.22	10.32 ± 0.34	N.D.	N.D.
Eu-BTC MOF	N.D.	N.D.	10.70	10.71 ± 0.12
$\text{Tb}_{0.5}\text{Eu}_{0.5}$ -BTC MOF	7.62	7.42 ± 0.53	8.55	8.52 ± 0.04
$\text{Tb}_{0.2}\text{Eu}_{0.8}$ -BTC MOF	2.44	2.23 ± 0.24	11.00	11.12 ± 0.11

the complex of Tb^{3+}/Eu^{3+} -EDTA complex, following by the characteristic emissions of Tb^{3+} and Eu^{3+} . The AuNPs can act as a catalyst for boosting the generation of 1O_2 in $NaO_4-H_2O_2$ system. Thanking to their narrow band emission of rare earth ions, simultaneous determination of Tb^{3+} and Eu^{3+} can be easily achieved at 490 nm and 620 nm, respectively. This sensing system with the merits of high sensitivity, selectivity as well as simplicity for the determination of Tb^{3+} and Eu^{3+} , provides a new avenue for multi-component CL analysis.

Declaration of competing interest

The authors declare no conflict of interest.

Acknowledgments

The authors gratefully acknowledge the financial support from the Sichuan Science and Technology Project (No. 2022NSFSC1087) and the Project of State Key Laboratory of Supramolecular Structure and Materials (No. sklssm2022034).

Supplementary materials

Supplementary material associated with this article can be found, in the online version, at doi:10.1016/j.ccl.2023.108155.

References

- [1] B. Li, Y. He, *Luminescence* 22 (2007) 317–325.
- [2] M. Liu, Z. Lin, J.M. Lin, *Anal. Chim. Acta* 670 (2010) 1–10.
- [3] L. Li, T. Yang, J. Yang, X. Zhang, *Sens. Actuator B: Chem.* 353 (2022) 131038.
- [4] S.N.A. Shah, X. Dou, M. Khan, K. Uchiyama, J.M. Lin, *Talanta* 196 (2019) 370–375.
- [5] Y. Sun, J. Lu, *Luminescence* 33 (2018) 1298–1305.
- [6] C. Wang, M.I. Halawa, B. Lou, et al., *Analyst* 146 (2021) 1981–1985.
- [7] Z. Li, Y. Xi, A. Zhao, et al., *Anal. Bioanal. Chem.* 413 (2021) 3541–3550.
- [8] C. Zhang, J. Jin, K. Liu, X. Ma, X. Zhang, *Chin. Chem. Lett.* 32 (2021) 3931–3935.
- [9] L. Li, D. Lin, F. Yang, et al., *ACS Appl. Nano Mater.* 4 (2021) 3932–3939.
- [10] W. Fan, L. Li, J. Yuan, et al., *Anal. Chem.* 93 (2021) 17043–17050.
- [11] J. Du, W. Liu, J. Lu, *Luminescence* 18 (2003) 341–345.
- [12] Q. Hu, S. Chen, F. Chen, *Spectrosc. Acta Part A: Molec. Biomolec. Spectr.* 264 (2022) 120332.
- [13] C. Pang, S. Han, Y. Li, J. Zhang, *J. Chin. Chem. Soc.* 65 (2018) 1504–1509.
- [14] C. Zhu, L. Wei, P. Yuan, L. Xiong, X. Cheng, *Instrum. Sci. Technol.* 45 (2016) 219–231.
- [15] Y. Li, Y.Z. Zheng, D.K. Zhang, et al., *Chin. Chem. Lett.* 28 (2017) 184–188.
- [16] S.N.A. Shah, A.H. Shah, X. Dou, et al., *ACS Omega* 4 (2019) 15004–15011.
- [17] P. Escribano, B. Julián-López, J. Planelles-Aragó, et al., *J. Mater. Chem.* 18 (2008) 23–40.
- [18] L.D. Carlos, R.A.S. Ferreira, V.d.Z. Bermudez, S.J.L. Ribeiro, *Adv. Mater.* 21 (2009) 509–534.
- [19] K. Binnemans, *Chem. Rev.* 109 (2009) 4283–4374.
- [20] X. Chen, Y. Xu, H. Li, *Dyes Pigment.* 178 (2020) 108386.
- [21] Y. Su, J. Yu, Y. Li, et al., *Commun. Chem.* 1 (2018) 1–12.
- [22] X. Zhou, T. Wang, M. Zhao, et al., *Sens. Actuator B: Chem.* 343 (2021) 130107.
- [23] H. Chen, W. Xue, C. Lu, et al., *Spectrosc. Acta Part A: Molec. Biomolec. Spectr.* 116 (2013) 355–360.
- [24] S. Cai, Y. Zhou, J. Ye, et al., *Microchim. Acta* 186 (2019) 463–475.
- [25] H. Song, Y. Su, L. Zhang, Y. Lv, *Luminescence* 34 (2019) 530–543.
- [26] H. Li, Y. Sun, Y. Li, J. Du, *Microchem. J.* 160 (2021) 105665.
- [27] Q. Li, M. Sun, Y. Su, K. Zhang, Y. Lv, *Sens. Actuator B: Chem.* 339 (2021) 129876.
- [28] X. Wang, H. Zhao, X. Li, S. Chen, *Chin. J. Anal. Chem.* 33 (2005) 647–649.
- [29] S. Chen, H. Zhao, X. Wang, X. Li, L. Jin, *Anal. Chim. Acta* 506 (2004) 25–29.
- [30] Y. Li, J. Wang, Y. Yang, S. Han, *Luminescence* 35 (2020) 773–780.
- [31] S.N. Shah, H. Li, J.M. Lin, *Talanta* 153 (2016) 23–30.
- [32] N. Sabbatini, M. Guardigli, J.M. Lehn, *Coord. Chem. Rev.* 123 (1993) 201–228.
- [33] G.F. de Sá, O.L. Malta, C. de Mello Donegá, et al., *Coord. Chem. Rev.* 196 (2000) 165–195.
- [34] Z.F. Zhang, H. Cui, C.Z. Lai, L.J. Liu, *Anal. Chem.* 77 (2005) 3324–3329.
- [35] S. Cai, K. Lao, C. Lau, J. Lu, *Anal. Chem.* 83 (2011) 9702–9708.
- [36] Y. Qi, B. Li, *Spectrosc. Acta Part A: Molec. Biomolec. Spectr.* 111 (2013) 1–6.
- [37] C. Huang, Y. Wang, Y. Wang, et al., *Appl. Surf. Sci.* 579 (2022) 151860.
- [38] J. Liu, H. Chen, L. Lin, C. Lu, J. Lin, *Chin. Sci. Bull.* 55 (2010) 3479–3484.
- [39] M. Zhang, D. Han, C. Lu, J.M. Lin, *J. Phys. Chem. C* 116 (2012) 6371–6375.
- [40] Z. Zhang, A. Berg, H. Levanon, R.W. Fessenden, D. Meisel, *J. Am. Chem. Soc.* 125 (2003) 7959–7963.
- [41] J. Rabani, S.O. Nielsen, *J. Am. Chem. Soc.* 73 (2002) 3736–3744.
- [42] T.Y. Huang, W.Y. Lin, *Luminescence* 26 (2011) 118–124.
- [43] J. Liu, H. Chen, Z. Lin, J.M. Lin, *Anal. Chem.* 82 (2010) 7380–7386.
- [44] Y. Zheng, D. Zhang, S.N.A. Shah, H. Li, J.M. Lin, *Chem. Commun.* 53 (2017) 5657–5660.